Synthesis and Characterization of Functionalized Triblock Polymer: The Prepared Polymer is Cholesteryl Terminated and Chain-Extended PCL

Jinbao Guo, Jie Sun, Hui Cao, Dongyu Zhao, Huai Yang

Department of Materials Physics and Chemistry, School of Materials Science and Engineering,
University of Science and Technology Beijing, Beijing 100083, People's Republic of China

Received 13 January 2007; accepted 9 April 2007
DOI 10.1002/app.26609

ABSTRACT: The functionalized triblock polymer for the preparation of self-assembly biomaterials, Chol-(CL)$_{\bar{n}}$-Chol, was synthesized through ring-opening polymerization of ε-caprolactone (ε-CL) following by chain-extension reaction. The chemical structure of functionalized triblock polymer was confirmed by Fourier transform infrared and ^{1}H-NMR. The molecular weight of the functionalized polymer increased with decreasing feed ratio of the initiator cholesterol (Chol) to the monomer ε-CL. Liquid crystalline properties and the self-assembly behavior of the functionalized polymer were validated by Wide angle X-ray diffraction, differential scanning calorimetry, and polarizing light microscope. The results showed that Chol-(CL)$_{\bar{n}}$-Chol ($\bar{n} \leq 40$) exhibited liquid crystallinity in particular temperature ranges because of the incorporation of the cholesteryl moiety. In addition, the functionalized triblock polymer can be homogeneously blended with high molecular weight poly(ε-caprolactone) (PCL), which offers the possibility to modify the properties of biomaterials based on PCL. Mixing a small amount of a Chol-(CL)$_{\bar{n}}$-Chol functionalized polymer with PCL, or coating a thin layer of the functionalized polymer on the surface of a PCL-based implant may modify cell response. © 2007 Wiley Periodicals, Inc. J Appl Polym Sci 105: 3505–3512, 2007

Key words: biodegradable; functionalization of polymers; self-assembly; liquid crystallinity; miscibility

INTRODUCTION

Biodegradable polymers represent an interesting class of biomaterials, which have received increased attention over the past few years. Among them, aliphatic polyesters are an important family of biodegradable polymers, such as polylactide (PLA),[1] polyglycolide,[2] poly(lactide-*co*-glycolide),[3] poly(ε-caprolactone) (PCL),[4–6] and poly(3-hydroxybutyrate).[7] Until now, much work has been carried out on the properties and applications of these polymers.[8–13] However, many properties of these polyesters fall short of the required properties for potential applications, for example, cell affinity toward these polyesters is generally poor as a consequence of their low hydrophilicity and lack of surface cell recognition sites.[10,11]

Many modification approaches have been used to optimize properties of these polyesters. Incorporation of the bioactive or biocompatible compounds including lipids, vitamins, hormones, and peptides to the polymer chain are one of the most important modification strategies.[12,13] Cholesterol (chol) moiety has been often chosen among them because of its high thermodynamic affinity for the cell membrane and its ability to change the membrane's permeability and fluidity.[14–19] Stupp and coworkers[15,16] reported that cholesteryl-oligo(L-lactic acid) obviously promoted cell adhesion and proliferation compared with poly(L-lactic acid). Later, Chen and cowworkers[17–19] described the use of cholesteryl end-capped polycarbonates and cholesteryl-PCL as drug release carrier. These successful results clearly illustrate that functionalization of polyesters by cholesteryl moiety hold promise as scaffold materials for drug release and tissue engineering.

Herein we described the synthesis and characterization of a novel set of biodegradable dicholesteryl functionalized triblock polymers (Chol-(CL)$_{\bar{n}}$-Chol), the different segments that constitute the dicholesteryl functionalized triblock polymers are either structurally important, or have functional relevance. It is well known that the liquid crystalline character of a series of cholesteryl esters has been found for a long time,[20–24] especially in recent years low molecular weight dicholesteryl esters attracted much attention as a new class of self-assembly materials.[25–29] Here, it was anticipated that the cholesteryl moiety could provide a driving force for the self assembly of the dicholesteryl functionalized triblock polymers.

Correspondence to: H. Yang (yanghuai@mater.ustb.edu.cn).
Contract grant sponsor: Ministry of Education of the People's Republic of China; contract grant number: 104187.

Journal of Applied Polymer Science, Vol. 105, 3505–3512 (2007)

What's more, the dicholesteryl functionalized triblock polymer also possesses some features that could make them of interest as molecular scaffolds for cell growth. In this article, the synthesis, molecular characterization, and self-assembly of dicholesteryl functionalized triblock polymers were described. In addition, the miscibility of triblock polymers with poly(ε-caprolactone) was studied.

EXPERIMENTAL

Materials

Cholesterol (Beijing chemical reagent, China) was purified by recrystallization from ethanol. ε-caprolactone (ε-CL, Aldrich) was distilled from CaH_2. Stannous octanoate ($Sn(Oct)_2$, Beijing Yili chemical reagent, China) was purified by distillation under reduced pressure and then dissolved in dry toluene prior to use. Hexamethylene diisocyanate (HDI) and poly(ε-caprolactone) (PCL, M_n = 42,500, M_w/M_n = 1.53) were purchased from Aldrich and PCL was dried in a vacuum oven at 100°C for 24 h. The other reagents and solvents were local commercial products and used without further purification.

Synthesis of triblock functionalized polymers

Chol-(CL)$_{\bar{n}}$-Chol triblock polymers were synthesized by two steps, at first Chol-(CL)$_{\bar{m}}$ diblock polymers were synthesized by the ring-opening polymerization of ε-caprolactone (ε-CL) using cholesterol (Chol) with a hydroxyl group as an initiator. Then Chol-(CL)$_{\bar{n}}$-Chol triblock polymers were obtained with HDI as crosslinker. The Chol/CL/Chol ratios for triblock polymers coded **1**, **2**, **3**, **4**, and **5** were 1 : 10 : 1, 1 : 14 : 1, 1 : 20 : 1, 1 : 40 : 1, and 1 : 50 : 1, respectively. For example, to synthesize the Chol-(CL)$_{\overline{10}}$-Chol, the cholesterol (3.86 g, 0.01 mol), ε-caprolactone (5.7 g, 0.05 mol), and stannous octoate (17 μL, 0.05 mmol) were added into well-dried three-neck flask with a magnetic stirring bar. The reaction mixtures were stirred at 140°C for 8 h. The progress of the reaction could be traced by the GPC chromatogram for this polymer. HDI (0.81 mL, 5 mmol) was added to the reaction mixture, and it was stirred at 60°C for 7 h. The product was isolated by precipitation into diethyl ether. The polymer was dissolved in 30 mL of methylene chloride and fractionally precipitated by slowly adding diethyl ether. The residual solvent was removed under vacuum.

Preparation of Chol-(CL)$_{\overline{40}}$-Chol/PCL blends

Three blends containing 20% (w/w) PCL, 50% (w/w) PCL, and 80% (w/w) were produced by a solution-evaporation technique respectively. Briefly, after preparing a 5% (w/v) triblock Chol-(CL)$_{\overline{40}}$-Chol polymer solution in methylene chloride (CH_2Cl_2) at 30°C, poly(ε-caprolactone) (PCL) was added to the solution and stirring was carried out for 1 h at 30°C. Then CH_2Cl_2 were evaporated by heating, dried in a vacuum oven at 40°C for 24 h. Dried samples were reduced into powders by milling in a mortar and pestle for analysis.

Instrument and measurement

Fourier transform infrared (FTIR) spectra were recorded on a Nicolet-510P spectrometer at frequencies ranging from 400 to 4000 cm^{-1}. Samples were thoroughly mixed with KBr and pressed into pellet form. Molecular weights and molecular weight distributions of the polymers were determined on a Waters HPLC system equipped with a 2690D separation module and a 2410 refractive index detector, THF as the eluent (1.0 mL/min). The differential scanning calorimetry (DSC) analysis was carried out using a Mettler DSC822e instrument under nitrogen flow (50 mL/min). All samples were heated and cooled at 10°C/min. Wide angle X-ray diffraction (WAXD) patterns of powder samples were obtained at room temperature on a Rigaku D_{max}-RB X-ray diffractometer with a Cu Ka radiation source (wavelength 1.54 Å). The supplied voltage and current were set to 40 kV and 150 mA, respectively. Samples were exposed at a scan rate of $2\theta = 2°$/min between $2\theta = 5°$ and 40°. The ^{1}H-NMR experiments were performed at 400.1, on a Bruker DMX-300 spectrometer. $CDCl_3$ was used as the deuterated solvents for the polymers. The polymers were observed by a polarizing light microscope (PLM; Olympus BX51) with a heating stage (LinkamTHMS-600). The samples were visualized using crossed polarizers. The optical images were recorded using Linksys 2.43 software.

RESULTS AND DISCUSSION

Synthesis and characterization of functionalized triblock polymer

Ring-opening polymerization is an efficient method for producing aliphatic polyesters with high molecular weights. For aliphatic cyclic esters, their ring-opening polymerizations can be carried out in the presence of initiators bearing hydroxyl groups.[15–19]In this investigation, Chol-(CL)$_{\bar{n}}$-Chol triblock polymer was synthesized by two steps. As shown in Scheme 1, first, the Chol-(CL)$_{\bar{m}}$ was synthesized by ring opening polymerization of ε-caprolactone (ε-CL) onto the Chol in the presence of stannous octoate as a catalyst. In this step, the reaction was carried out under rigorous anhydrous conditions. The chol and

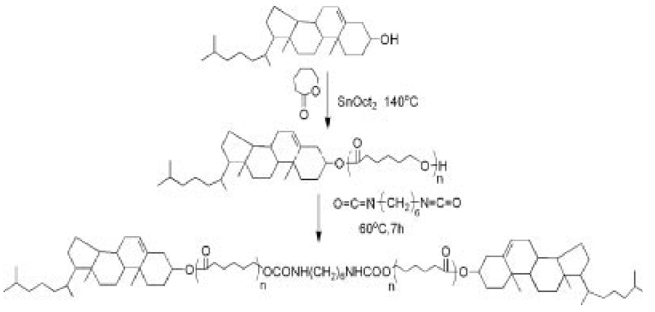

Scheme 1 Synthesis of Chol-$(CL)_{\bar{n}}$-Chol.

the monomer CL were carefully dried to avoid the initiation by water, which induces a mixture of PCL and Chol-$(CL)_{\bar{m}}$. The optimized polymerization conditions were identified to be 8 h at 140°C. Under this condition, the monomers can be efficiently initiated by the OH group of chol and yield Chol-$(CL)_{\bar{m}}$ after the polymerization. Second, the Chol-$(CL)_{\bar{m}}$ diblock polymer with a terminal hydroxyl group was coupled by HDI to the Chol-$(CL)_{\bar{n}}$-Chol triblock polymer, this reaction had a very high yield because the —NCO group of HDI was easy to react with —OH group of Chol-$(CL)_{\bar{m}}$. The chemical structure of Chol-$(CL)_{\bar{n}}$-Chol triblock polymer was verified by FTIR and ^{1}H-NMR. The progress of the reaction, that is, Chol-$(CL)_{\bar{m}}$ diblock polymer, and Chol-$(CL)_{\bar{n}}$-Chol triblock polymer, could be traced by gel permeation chromatography (GPC).

The chemical structure of the Chol-$(CL)_{\bar{n}}$-Chol was verified by FTIR. As a typical example, the FTIR spectra for Chol-$(CL)_{\overline{40}}$-Chol was shown in Figure 1, the band at 1724 cm^{-1} was attributed to C=O in Chol-$(CL)_{\overline{40}}$-Chol repeating units as well as in Chol-$(CL)_{\overline{20}}$. And the weak absorption peak at 1630 cm^{-1} which comes from C=C of cholesteryl moiety both in the spectra of Chol-$(CL)_{\overline{20}}$ [Fig. 1(b)] and that of Chol-$(CL)_{\overline{40}}$-Chol [Fig. 1(c)] was also found. In addition, the spectrum of Chol-$(CL)_{\overline{40}}$-Chol shown a broad band at 3387 cm^{-1}, which belongs to N—H stretching vibration, the presence of C—N was supported by the absorption peak at 1530 cm^{-1}. These indicated that HDI was present in Chol-$(CL)_{\overline{40}}$-Chol.

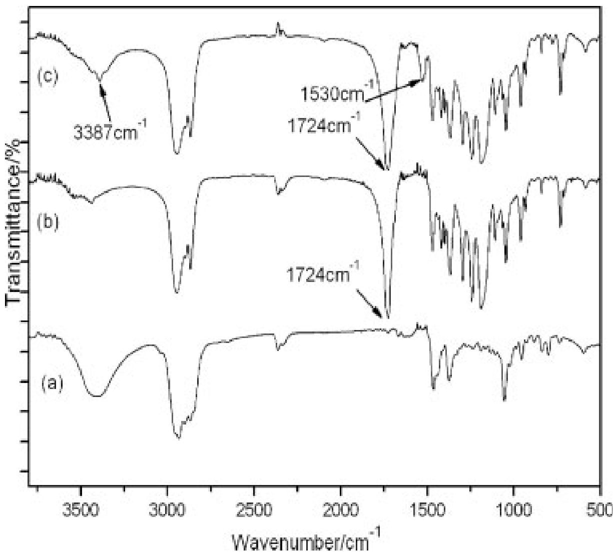

Figure 1 FTIR spectra of (a) cholesterol; (b) Chol-$(CL)_{\overline{20}}$; and (c) Chol-$(CL)_{\overline{40}}$-Chol.

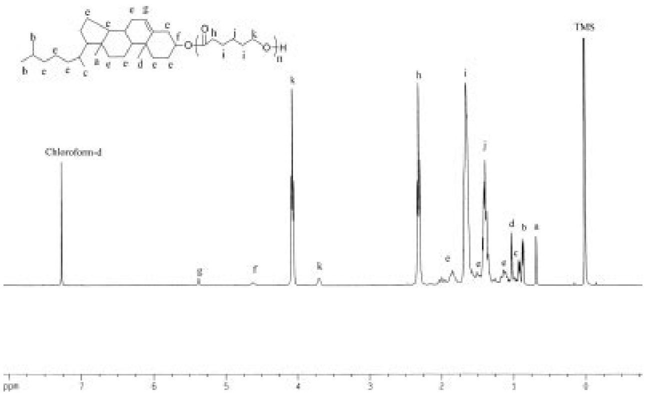

Figure 2 ^{1}H-NMR spectra of Chol-$(CL)_{\overline{20}}$.

Figures 2 and 3 showed the ^{1}H-NMR spectra of Chol-$(CL)_{\overline{20}}$ and Chol-$(CL)_{\overline{40}}$-Chol, respectively. The typical signals of the cholesteryl moiety and CL repeating units can be observed both in the spectrum of Chol-$(CL)_{\overline{20}}$ and that of Chol-$(CL)_{\overline{40}}$-Chol at 0.67, 0.85, 0.87, 0.98 ppm (cholesteryl moiety: —$\boldsymbol{CH_3}$), 5.34 ppm (cholesteryl moiety: —$\boldsymbol{CH}$=C), 4.58 ppm (cholesteryl moiety: —$\boldsymbol{CH}$OCO), and 1.35(—OCH$_2$CH$_2$$\boldsymbol{CH_2}CH_2CH_2$CO—), 1.62(—OCH$_2$$\boldsymbol{CH_2}$ CH$_2$—$\boldsymbol{CH_2}$CH$_2$CO—), 2.30 (—OCH$_2$CH$_2$CH$_2$CH$_2$$\boldsymbol{CH_2}$ CO—), 4.06 (—O$\boldsymbol{CH_2}$CH$_2$CH$_2$CH$_2$CH$_2$CH$_2$CO—). Because the Chol-$(CL)_{\overline{20}}$ diblock polymer with a terminal hydroxyl group was coupled by HDI to the Chol-$(CL)_{\overline{40}}$-Chol triblock polymer, the signal at 3.64 ppm for Chol-$(CL)_{\overline{20}}$ (—C$\boldsymbol{H_2}$OH) could not be found in the spectrum of Chol-$(CL)_{\overline{40}}$-Chol anymore, and a

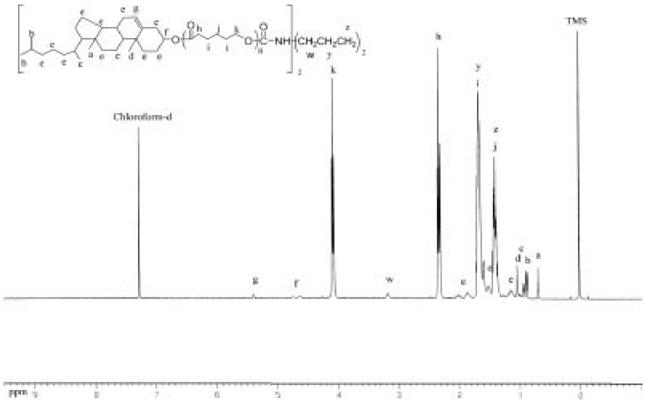

Figure 3 ^{1}H-NMR spectra of Chol-$(CL)_{\overline{40}}$-Chol.

TABLE I
Synthesis and Molecular Weights of Triblock Polymers

Polymer	Chol/CL/Chol feed ratio (mol/mol)	Yield (%)	M_n[a]	M_w[a]	M_w/M_n
1	1 : 10 : 1	50	2,645	3,957	1.49
2	1 : 14 : 1	58	3,965	5,250	1.33
3	1 : 20 : 1	65	6,092	8,029	1.31
4	1 : 40 : 1	72	10,920	15,413	1.41
5	1 : 50 : 1	86	12,256	19,865	1.62

[a] Determined by GPC. In the GPC, tetrahydrofuran (THF) was used as an eluting solvent and PSs in a molecular weight range of 400–10,0000 were used as the molecular weight standards.

new signal appeared at 3.13 ppm (HDI moiety: —OOCNH$\boldsymbol{CH_2}$CH$_2$CH$_2$CH$_2$—CH$_2$$\boldsymbol{CH_2}$NHCOO—) in the spectrum of Chol-(CL)$_{\overline{40}}$-Chol in Figure 3. From earlier analysis, it can be concluded that the synthesis of Chol-(CL)$_{\bar{n}}$-Chol was well controlled.

The GPC data of the triblock polymer were listed in Table I, in this study, a series of triblock polymers with different molecular weights were synthesized. As shown in Table I, the molecular weight of Chol-(CL)$_{\bar{n}}$-Chol increased with decreasing Chol/CL feed ratio. GPC results also showed that all functionalized triblock polymers prepared have unimodal molecular weight distributions, and the M_w/M_n values of triblock polymer were relatively narrow in the range of 1.31–1.62. Figure 4 showed the typical GPC curves of the triblock polymer Chol-(CL)$_{\overline{40}}$-Chol and diblock intermediate Chol-(CL)$_{\overline{20}}$. Both of them showed a unimodal distribution with little change in the molecular weight distribution. However, the peak of the Chol-(CL)$_{\overline{40}}$-Chol shifted toward a higher molecular weight region in comparison with the peak of Chol-(CL)$_{\overline{20}}$ given in Figure 4, suggesting diblock polymer Chol-(CL)$_{\overline{20}}$ should be coupled by HDI to triblock polymer Chol-(CL)$_{\overline{40}}$-Chol. As mentioned earlier, by controlling the reaction condition rigorously, the monomers can be efficiently initiated by the OH group of chol, PCL homopolymer can be limited by maximum degrees in the first step. Additionally, owing to the high reactivity of —NCO group with —OH group, a well-defined structure of the functionalized triblock polymer can be achieved. In all, these results indicated that the functionalized triblock polymer can be synthesized successfully by ring-opening polymerization of ε-caprolactone following by chain-extension reaction.

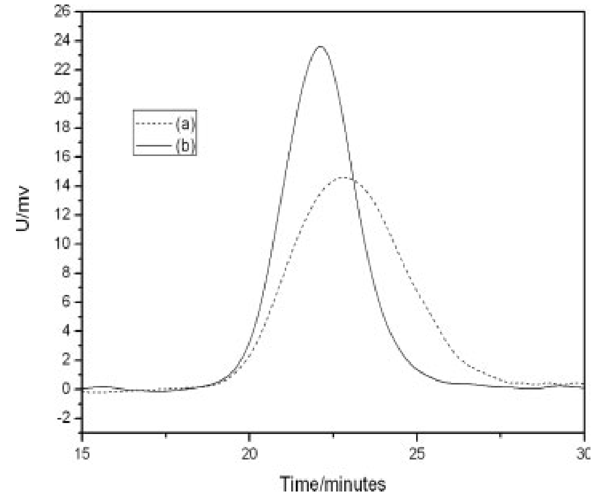

Figure 4 GPC chromatogram of (a) Chol-(CL)$_{\overline{20}}$ diblock polymer and (b) Chol-(CL)$_{\overline{40}}$-Chol triblock polymer.

Liquid crystallinity induced by the cholesteryl moiety

It is well known that cholesteryl moiety has mesogenic nature,[14] triblock polymers with certain molecular weights should exhibit liquid crystallinity in particular temperature ranges. To examine the liquid crystallinity of Chol-(CL)$_{\bar{n}}$-Chol, the samples of different molecular weight triblock polymers were characterized by DSC, PLM, and WAXD. The results were shown in Figures 5–7 and Table II. As shown in Table II, the samples Chol-(CL)$_{\overline{10}}$-Chol-**1**, Chol-(CL)$_{\overline{14}}$-Chol-**2**, Chol-(CL)$_{\overline{20}}$-Chol-**3**, and Chol-(CL)$_{\overline{40}}$-Chol-**4** displayed liquid crystal textures in certain temperature ranges. For triblock polymer Chol-(CL)$_{\overline{50}}$-Chol-**5**, with very low cholesteryl content, no obvious liquid crystalline state can be observed.

TABLE II
Phase Transition Temperatures of Chol-(CL)$_{\bar{n}}$-Chol

Polymer	Temperature range in which liquid crystallinity is exhibited[a] (°C)	T_c[b] (°C)
Chol-(CL)$_{\overline{10}}$-Chol-1	37–53	does not crystallize
Chol-(CL)$_{\overline{14}}$-Chol-2	47–54	−2
Chol-(CL)$_{\overline{20}}$-Chol-3	51–56	12
Chol-(CL)$_{\overline{40}}$-Chol-4	54–58	24
Chol-(CL)$_{\overline{50}}$-Chol-5	no obvious liquid crystallinity	27

[a] Temperature range in which liquid crystallinity was exhibited was determined by PLM.
[b] T_c was determined by DSC.

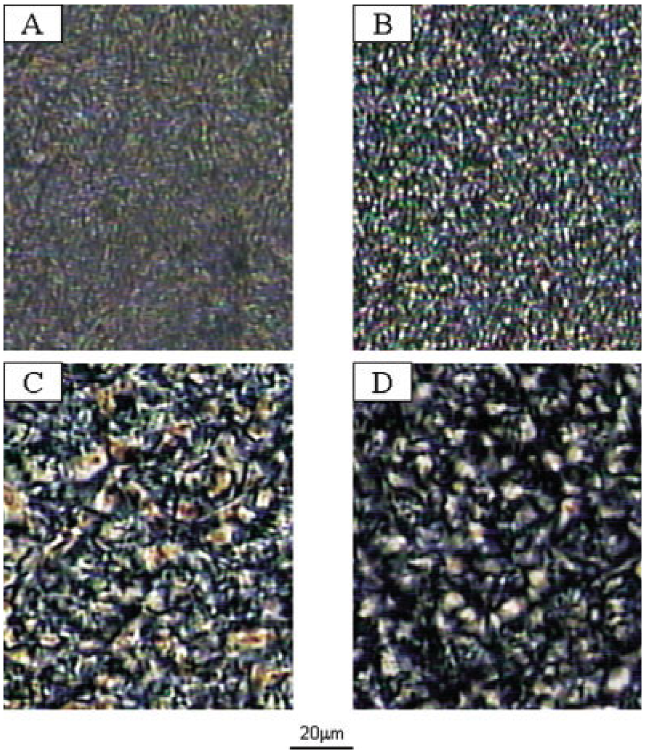

Figure 5 PLM images of Chol-(CL)$_{\overline{40}}$-Chol-**4** (×400) during the second heating (A) 20°C; (B) 35°C; (C) 54°C; and (D) 56°C. [Color figure can be viewed in the online issue, which is available at www.interscience.wiley.com.]

From PLM characterization, it can be found that Chol-(CL)$_{\overline{10}}$-Chol-**1** showed a transition of solid state to liquid crystalline state at 37°C and a transition of liquid crystalline state to isotropic state at 53°C. Similar phenomena can be observed for Chol-(CL)$_{\overline{14}}$-Chol-**2**, Chol-(CL) $_{\overline{20}}$-Chol-**3**, and Chol-(CL)$_{\overline{40}}$-Chol-**4**. What's more with an increase in molecular weight, the transition temperature increased and the temperature range in which liquid crystallinity exhibited become narrow. From earlier results, it seemed that the chain length of poly(ε-caprolactone) plays an important role in determining the morphology of triblock polymers.

Herein, as a representative example, the textures of Chol-(CL)$_{\overline{40}}$-Chol-**4** with the temperature changing were given in Figure 5. From figures it can be seen that the sample was unconspicuous spherocrystal at room temperature [Fig. 5(A)]; when heated to 35°C, it still kept crystallization [Fig. 5(B)], crystallites with smaller size can also be seen. When the sample was heated at 54°C, the birefringence could be observed [Fig. 5(C)]. Especially at 56°C, it can be observed that the birefringence become very obvious [Fig. 5(D)], which is similar to the texture of cholesteric phase. When the sample was heated to 58°C, the birefringence disappeared, that indicated the mesophase transfered to the isotropic phase.

As it is well known, typically a solid–liquid crystal transition peak and a liquid crystal–isotropic transition peak should appear during heating and cooling of low molecular-weight liquid crystal with a well-defined structure, such as low molecular weight dicholesteryl esters.[26,29] However, in this investigation, only one peak was detected during heating and cooling in DSC curves (Fig. 6), although the PLM results displayed an obvious birefringence character, which is very similar to that of the other functionalized polymers/oligomers by chol moiety.[17,18] The possible reason for this is that the polydispersity of the polymers. The transition peaks may overlap each other, so the overall DSC curve only showed a single peak. However, a clear trend from the DSC results was still found. Because of the strong crystallizibility of the PCL chain, except for Chol-(CL)$_{\overline{10}}$-Chol-**1**, crystallization peaks appeared during cooling of

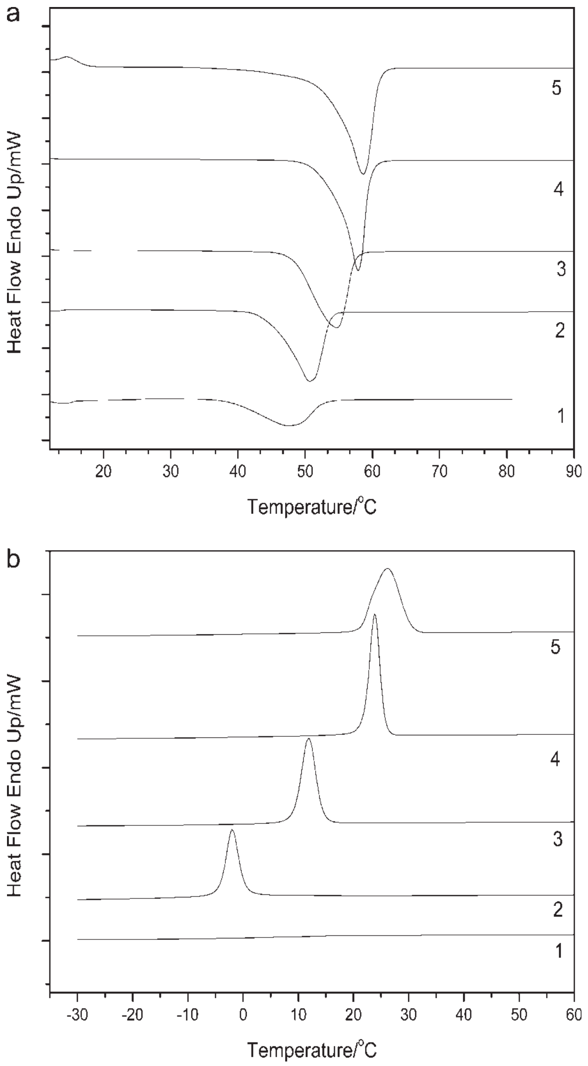

Figure 6 (A) DSC first heating scans of Chol-(CL)$_{\bar{n}}$-Chol. (Chol-(CL)$_{\overline{10}}$-Chol-**1**; Chol-(CL)$_{\overline{14}}$-Chol-**2**; Chol-(CL)$_{\overline{20}}$-Chol-**3**; Chol-(CL)$_{\overline{40}}$-Chol-**4**; and Chol-(CL)$_{\overline{50}}$-Chol-**5**) (B) DSC first cooling scans of Chol-(CL)$_{\bar{n}}$-Chol.

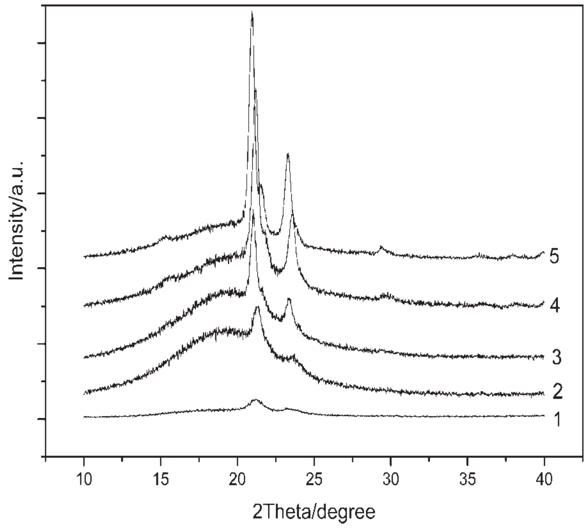

Figure 7 WAXD patterns of Chol-(CL)$_{\overline{n}}$-Chol measured at 25°C. (Chol-(CL)$_{\overline{10}}$-Chol-**1**; Chol-(CL)$_{\overline{14}}$-Chol-**2**; Chol-(CL)$_{\overline{20}}$-Chol-**3**; Chol-(CL)$_{\overline{40}}$-Chol-**4**; and Chol-(CL)$_{\overline{50}}$-Chol-**5**)

samples Chol-(CL)$_{\overline{14}}$-Chol-**2**, Chol-(CL)$_{\overline{20}}$-Chol-**3**, and Chol-(CL)$_{\overline{40}}$-Chol-**4**. What's more, the crystallization temperature (T_c) increased with increasing chain length of PCL. In other words, T_c decreased with increasing cholesteryl content in the polymer.

Figure 7 showed the WAXD patterns of Chol-(CL)$_{\overline{n}}$-Chol measured at 25°C. Except for Chol-(CL)$_{\overline{10}}$-Chol-**1**, all other Chol-(CL)$_{\overline{n}}$-Chol exhibited two crystalline peaks appearing at 2θ equal to 21° and 23°, corresponding to reflections of orthorhombic PCL crystals, respectively. This indicated that the crystal structure of PCL in Chol-(CL)$_{\overline{n}}$-Chol was similar to that of high molecular weight PCL homopolymer. Crystallinity of PCL in Chol-(CL)$_{\overline{n}}$-Chol increased dramatically with increasing the chain length of PCL. From the earlier observation and analysis it could be concluded that in Chol-(CL)$_{\overline{10}}$-Chol-**1** where PCL is amorphous, the LC moiety was found to be dominant in determining morphology. In Chol-(CL)$_{\overline{14}}$-Chol-**2**, Chol-(CL)$_{\overline{20}}$-Chol-**3**, and Chol-(CL)$_{\overline{40}}$-Chol-**4**, LC and crystalline phases coexisted and competed of each other, only in particular temperature ranges they exhibit liquid crystallinity. For Chol-(CL)$_{\overline{50}}$-Chol-**5** with further increase in the chain length of PCL, the crystalline PCL become dominant in determining morphology and the LC phase was not detected. This phenomenon and result were similar to that of poly(oxyethylene) chol ethers.[30]

Miscibility and crystallization behavior of Chol-(CL)$_{\overline{40}}$-Chol/PCL blends

In this research, we studied the miscibility and crystallization behavior of earlier triblock polymer blending with the high molecular weight poly(ε-caprolactone) (PCL). It is well known that miscibility between the two components plays an important role on the morphology, thermal properties, and biodegradability.[31–35] Here, blends were prepared by solution mixing of a certain amount of PCL with Chol-(CL)$_{\overline{40}}$-Chol followed by evaporation of the solvent, and were subsequently investigated by means of DSC and WAXD. DSC heating traces and WAXD scans were shown in Figures 8 and 9 for several blends of PCL/Chol-(CL)$_{\overline{40}}$-Chol.

Figure 8 showed DSC first heating scans for all the investigated Chol-(CL)$_{\overline{40}}$-Chol/PCL blends. Three blends with different weight ratio (20%, 50%, 80%) for all the investigated Chol-(CL)$_{\overline{40}}$-Chol/PCL revealed only one melting temperature (T_m) in the DSC thermograms, no other endotherm was observed, indicating miscibility of both components of the blends. In addition, blending affects at some extent the component crystallinity degree and T_c (or T_m).[31] The effect was pronounced for Chol-(CL)$_{\overline{40}}$-Chol/PCL blends. As shown in Figure 8, the T_m of Chol-(CL)$_{\overline{40}}$-Chol/PCL blend gradually shifted from 57.8°C for pure Chol-(CL)$_{\overline{40}}$-Chol to 63.9°C for the pure PCL, that is to say, the T_m of Chol-(CL)$_{\overline{40}}$-Chol/PCL blend become high with the PCL content increasing.

The WAXD results shown in Figure 9 indicated a high level of order on a molecular scale for all the investigated Chol-(CL)$_{\overline{40}}$-Chol/PCL blends. Throughout the range of investigated compositions, clear WAXD peaks were observed, which did not significantly broaden with increasing amounts of PCL. Pure Chol-(CL)$_{\overline{40}}$-Chol, pure PCL and blends displayed their main peaks at 2θ equal to 21° and 23°

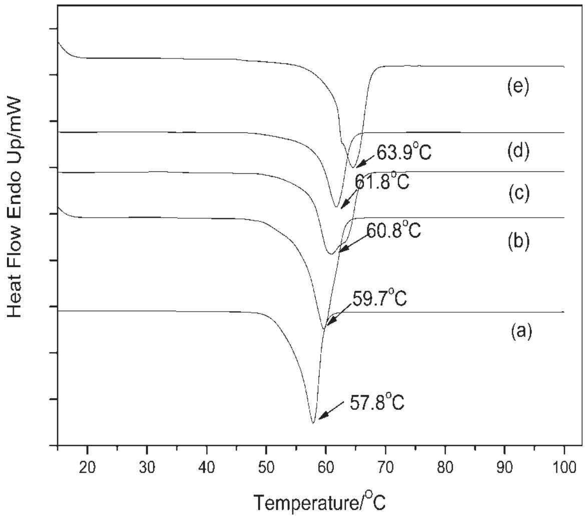

Figure 8 DSC heating traces of several blends of (a) Chol-(CL)$_{\overline{40}}$-Chol; (b) 20%PCL; (c) 50%PCL; (d) 80%PCL; and (e) PCL.

in Figure 9, which were those typical of an orthorhombic crystalline unit cell.

Optical microscopy observations carried out on film samples obtained from sample powders for investigating the miscibility and crystallization of the blends, thin films obtained by sandwiching particles among a glass slide, and a cover glass at 65°C for 3 min, followed by cooling at room temperature. From Figure 10, it can be observed that there was no obvious phase separation for all the blends, it is obvious that a high level of miscibility on a molecular scale happened for all the investigated Chol-(CL)$_{\overline{40}}$-Chol/PCL blends. In addition, large spherulites with 30–50 μm diameter were observed for pure PCL [Fig. 10(D)], whereas crystallites with smaller size and irregular shape were found for three blends [Figs. 10(A-C)], which suggests that crystallinity degree of PCL was affected by blending, this is in accordance with DSC results.

The miscibility of Chol-(CL)$_{\bar{n}}$-Chol with high molecular weight PCL offers the possibility to improve the properties of biomaterials based on PCL. For example, cell response of earlier biomaterials can be modified by coating a thin layer of the functionalized polymer on the surface of a preformed PCL-based implant, or mixing a small amount of Chol-(CL)$_{\bar{n}}$-Chol with PCL prior to the final processing step.

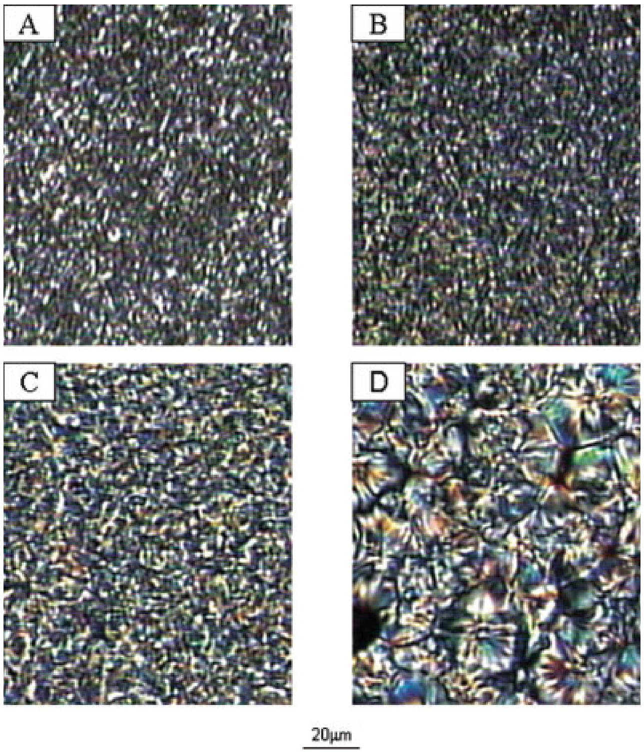

Figure 10 Optical microscopy images (×400) of (A) 20%PCL; (B) 50%PCL; (C) 80%PCL; and (D) PCL. [Color figure can be viewed in the online issue, which is available at www.interscience.wiley.com.]

CONCLUSIONS

In this study, a new series of novel functionalized triblock polymers were successfully synthesized by ring opening polymerization of ε-caprolactone following by chain-extension reaction. The structure was confirmed by FTIR and ^{1}H-NMR. The obtained Chol-(CL)$_{\bar{n}}$-Chol ($\bar{n} \leq 40$) triblock polymers showed liquid crystallinity due to incorporation of the cholesteryl moiety, for Chol-(CL)$_{\bar{n}}$-Chol ($\bar{n}$ = 10, 14, 20, and 40), the solid–liquid crystal transition temperature increased and the ranges of the liquid crystallinity temperature become narrow with an increase in molecular weight. Furthermore, functionalized triblock polymers can be homogeneously mixed with high molecular weight PCL, which was validated by DSC, WAXD, and PLM, the miscibility offers the possibility to modify the properties of biomaterials based on PCL that are already approved for human use.

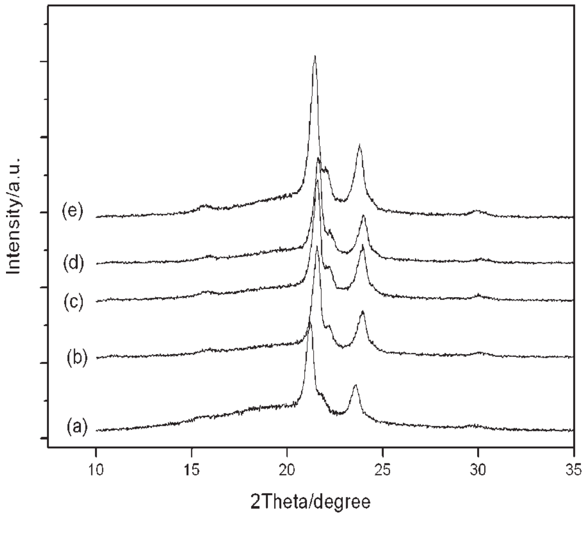

Figure 9 WAXD patterns recorded at 25°C of several blends of (a) Chol-(CL)$_{\overline{40}}$-Chol; (b) 20%PCL; (c) 50%PCL; (d) 80%PCL; and (e) PCL.

The authors thank Dr Zhaoguo Jin for his technical assistance in the differential scanning calorimetry (DSC) experiments and Mrs Lin Shi for her help with the polarizing light microscope (PLM).

References

1. Yamashita, K.; Kikkawa, Y.; Kurokawa, K.; Doi, Y. Biomacromolecules 2005, 6, 850.
2. Sahoo, S. K.; Panda, A. K.; Labhasetwar, V. Biomacromolecules 2005, 6, 1132.
3. Jain, R. A. Biomaterials 2000, 21, 2475.
4. Sinha, V. R.; Bansal, K.; Kaushik, R.; Kumria, R.; Trehan, A. Int J Pharm 2004, 278, 1.

5. Ponsart, S.; Coudane, J.; Vert, M. Biomacromolecules 2000, 1, 275.
6. Coombes, A. G. A.; Rizzi, S. C.; Williamson, M.; Barralet, J. E.; Downes, S.; Wallace, W. A. Biomaterials 2004, 25, 315.
7. Sun, J. Y.; Wu, J.; Li, H. Y.; Chang, J. Eur Polym J 2005, 41, 2443.
8. Hu, Y. F.; He, Y.; Wei, J; Li, S. M. J Appl Polym Sci 2007, 103, 2451.
9. Kim, E. G.; Kim, B. S.; Kim, D. S. J Appl Polym Sci 2007, 103, 928.
10. Cai, Q.; Wan, Y.; Bei, J.; Wang, S. Biomaterials 2003, 24, 3555.
11. Cai, Q.; Wan, Y.; Bei, J.; Wang, S. Biomaterials 2002, 23, 4483.
12. Yuan, W. Z.; Yuan, J. Y.; Huang, X. B.; Tang, X. Z. J Appl Polym Sci 2007, 104, 2310.
13. Meng, S.; Zhong, W.; Du, Q. G. J Appl Polym Sci 2007, 103, 989.
14. Urata, K.; Takaishi, N. Eur J Lipid Sci Technol 2001, 103, 29.
15. Klok, H. A.; Hwang, J. J.; Hartgerink, J. D.; Stupp, S. I. Macromolecules 2002, 35, 746.
16. Hwang, J. J.; Iyer, S. N.; Li, L. S.; Claussen, R.; Harrington, D. A.; Stupp, S. I. Proc Natl Acad Sci USA 2003, 99, 9662.
17. Wan, T.; Zou, T.; Cheng, S. X. Biomacromolecules 2005, 6, 524.
18. Zhang, L.; Wang, Q. R.; Jiang, X. S.; Cheng, S. X.; Zhuo, R. X. J Biomater Sci Polym Ed 2005, 9, 1195.
19. Yu, L.; Zhang, H.; Cheng, S. X.; Zhuo, R. X.; Li, H. J Biomed Mater Res Part B: Appl Biomater 2006, 77B, 39.
20. Weiss, R. G. Tetrahedron 1988, 44, 3413.
21. Yelamaggad, C. V.; Nagamani, A. S.; Hiremath, U. S.; Nair, G. G. Liq Cryst 2001, 28, 1009.
22. Goodby, J. W. Liq Cryst 1998, 24, 25.
23. Kim, K. N.; Do, E. D.; Kwon, Y. W.; Jin, J. I. Liq Cryst 2005, 32, 229.
24. Lee, W. K.; Kim, K. N.; Achard, M. F.; Jin, J. I. J Mater Chem 2006, 16, 2289.
25. Tamaoki, N.; Moriyama, M.; Matsuda, H. Angew Chem Int Ed 2000, 3, 509.
26. Tamaoki, N.; Kruk, G.; Matsuda, H. J Mater Chem 1999, 9, 2381.
27. Tamaoki, N.; Purfenov, A. V.; Masaki, A.; Matsuda, H. Adv Mater 1997, 9, 1102.
28. Jung, J. H.; Shinkai, S.; Shimizu, T. Chem Mater 2003, 15, 2141.
29. Kruk, G.; Tamaoki, N.; Matsuda, H.; Kida Y. Liq Cryst 1999, 26, 1687.
30. Xu, J. T.; Xue, L.; Fan, Zh. Q.; Wu, Zh. H.; Kim, J. K. Macromolecules 2006, 39, 2981.
31. Ciardelli, G.; Chiono, V.; Vozzi, G. Biomacromolecules 1961 2005, 6.
32. Madbouly, S. A. J Appl Polym Sci 2007, 103, 3307.
33. Ma, G. L.; Song, C. X. J Appl Polym Sci 2007, 104, 1895.
34. Ho, R. M.; Chiang, Y. W. Macromolecules 2002, 35, 1299.
35. Na, Y. H.; He, Y.; Shuai, X. T.; Kikkawa, Y.; Doi, Y.; Inoue, Y. Biomacromolecules 2002, 3, 1179.